Diclazuril-induced expression of CDK-related kinase 2 in the second-generation merozoites of Eimeria tenella

Bian-hua Zhou (zhoubh@haust.edu.cn)
Henan University of Science and Technology https://orcid.org/0000-0003-3811-3898
Hai-yan Ding
Henan University of Science and Technology
Jing-yun Yang
Henan University of Science and Technology
Jun Chai
Luoyang Polytechnic
Hong-wei Guo
Henan University of Animal Husbandry and Economy
Er-jie Tian
Henan University of Science and Technology

Research article

Keywords: CRK2, Diclazuril, cell cycle, Eimeria tenella

Posted Date: January 19th, 2021

DOI: https://doi.org/10.21203/rs.3.rs-28965/v2

Abstract

Background: Diclazuril is a classic anticoccidial drug. The key molecules of diclazuril in anticoccidial action allows target screening for the development of anticoccidial drugs. In the present study, a diclazuril anticoccidiosis animal model was established, and the transcription and translation levels of the CDK-related kinase 2 of *Eimeria tenella* (*Et*CRK2) were detected through quantitative real-time PCR and Western blot analysis, respectively. The localisation of *Et*CRK2 in merozoites was examined with immunofluorescence techniques.

Results: The mRNA and protein expression levels of *Et*CRK2 decreased in the infected/diclazuril group compared with those in the infected/control group. In addition, immunofluorescence analysis showed that *Et*CRK2 was localised in the cytoplasm of the merozoites. The fluorescence intensity of *Et*CRK2 in the infected/diclazuril group was significantly weaker than that in the infected/control group.

Conclusions: The anticoccidial drug diclazuril against *E.tenella* affects the expression pattern of *Et*CRK2 molecule, and *Et*CRK2 is a potential target for new drug development.

Background

Eimeria tenella is an obligate intracellular parasite that invades chicken caecal epithelial cells to survive and complete its lifecycle. This parasite causes a serious form of coccidiosis and huge economic losses to the poultry community [1]. The prevention and control of coccidiosis mainly rely on chemical drugs. However, coccidial resistance is induced by the long-term use of anticoccidiosis drugs [2]. Therefore, novel drug targets and control strategies must be sought.

E. tenella has a complex lifecycle that involves an asexual stage (sporogony and schizogamy) and a sexual stage (gametogony) [3]. During schizogamy, under the precise regulation of cell cycle, *E. tenella* proliferates rapidly within host cells [4]; this process is similar to cell cycles in other eukaryotes regulated by cyclin-dependent kinases (CDKs) [5]. Cyclin-dependent kinases (CDKs) are serine/threonine kinases that regulate the activity of substrate proteins through phosphorylation [6, 7], which regulates cell cycle progression, proliferation and differentiation and modulates transcription [8-13]. Several CDK-like kinases have been identified and characterised in parasitic protozoans. *Toxoplasma gondii* CRK1 (TgCRK1), TgCRK2, TgCRK4 and TgCRK6 are essential for tachyzoite replication and growth [14]. *Plasmodium falciparum* CDK-related kinase 3 (PfCRK-3) plays a key role in the intraerythrocytic development of *P. falciparum* [15]. *Plasmodium berghei* CDK-related kinase 5 (CRK5) is necessary for the S- and M- phases during gametogony and is required for mosquito transmission [16]. *Theileria annulata* CRK3 may be a regulator in gene transcription in all bovine intracellular life cycle stages [17]. CDK2 is involved in the differentiation of *Giardia lamblia* into cysts [8]. CDK-related kinase 2 (*Et*CRK2) is the only CDK that has been confirmed in *E. tenella*. It is expressed during the asexual and sexual states of *E. tenella* development [5, 18]. *E. tenella* schizont development is completely inhibited under treatment with the special CDK inhibitor flavopiridole at concentrations of 150 and 300 nM. Thus, *E. tenella* CDKs are

considered chemically validated drug targets [4, 5]. In our previous study, *Et*CDK was found to have differential expression according to the diclazuril anticoccidial cDNA library constructed through the suppression of subtractive hybridisation (data not shown). We investigated the expression pattern of *Et*CRK2 in response to diclazuril treatment against *E. tenella* infection.

Diclazuril, a classic anticoccidial drug, significantly induces merozoite apoptosis, effectively decreases the number of merozoites, and alleviates cecum damage induced by *E. tenella* [19-24]. Here, we reported changes in *Et*CRK2 in response to diclazuril treatment against *E. tenella* infection and observed the expression levels of *Et*CRK2 mRNA and protein and the spatial location of *Et*CRK2.

Results

Cloning of the *Et*CRK2 gene

The 1015 bp *Et*CRK2 gene was amplified from second-generation merozoites and cloned into a pMD-19T vector. A DNA fragment of *Et*CRK2 ORF amplified from pMD-19-*Et*CRK2 was subcloned into pET-28a (+). The recombinant plasmid pET-28a-*Et*CRK2 was analysed through PCR with pET-28a (+) vector universal primers, and the product length was in accordance with ORF 891 bp plus vector sequence 360 bp (Fig. 1). A 891 bp insertion ORF was also identified by *Eco*R I and *Hin*d III enzyme digestion (Fig. 2) and sequenced for 100% correctness.

Expression of recombinant *Et*CRK2 protein and polyclonal preparation

A high level of r*Et*CRK2 protein expression was achieved by inducing the r*Et*CRK2 protein at 37 °C with 0.5 mM IPTG for 4 h. The protein was then separated through SDS-PAGE (Fig. 3). The theoretical molecular weight of the r*Et*CRK2 protein was approximately 37.67 kDa. The purified r*Et*CRK2 protein (Fig. 4) was used for antibody preparation. The antiserum had a specific binding with the recombinant protein (Fig. 5), and the titer of the antibody against r*Et*CRK2 exceeded 1:512K (Fig. 6).

Expression of *Et*CRK2 mRNA

Fig. 7 shows that the mRNA expression level of *Et*CRK2 in the infected/diclazuril group was downregulated by 42.3% relative to that in the infected/control group ($P < 0.01$).

Western blot analysis

As shown in Fig. 8, the *Et*CRK2 protein expression level in the infected/diclazuril group was downregulated by 59.32% ($P < 0.01$) relative to that in the infected/control group.

Immunofluorescence analysis

The subcellular location of *Et*CRK2 in the second-generation merozoites was visualised through immunofluorescence microscopy. As shown in Fig. 9, *Et*CRK2 was widely distributed in the cytoplasm of

the merozoites. The green fluorescence in the merozoites of the infected/diclazuril group was darker than that in the merozoites of the infected/control group.

Discussion

Coccidiosis caused by the apicomplexan parasites of the genus *Eimeria* induces high

economic problems by reducing poultry productivity and performance [25]. *E. tenella*

is one of the most virulent species of *Eimeria*, mainly infects the chicken cecum. During second-generation schizogony, large amounts of released second-generation merozoites reinvade other uninfected caecal epithelial cells. Therefore, inhibiting the reproductive process of second-generation merozoites may be an effective strategy for controlling coccidiosis.

E. tenella utilises complex and distinctive mechanisms to regulate its replicative cycles [14]. CDKs participates in mediating cell proliferation and division in the parasite [7, 26-28]. In *Plasmodium berghei*, CRK2 mRNA is highly expressed in gametocytes and mosquito endophase; this characteristic suggests that CRK2 protein has a key role throughout the life cycle [29]. At the trophozoite/schizont stage, the inhibition of *P. falciparum* Cdc2-related kinase-1 (PfCRK-1) protein interferes with the schizogony of *P. falciparum* [30]. The depletion of *Plasmodium falciparum* CRK4 results in the complete blockage of nuclear division and intensively inhibits DNA replication during schizogony in the intraerythrocytic blood stage [31]. The downregulation of *P. falciparum* MO15-related protein kinase, Cdc2-related kinase PfPK5, *P. falciparum* CRK3 and other cyclins during dormancy arrests parasite progression at the G_1 phase and halts DNA synthesis [32]. The loss of cytoplasmic TgCRK2 results in *T. gondii* cell cycle G1 phase arrest [14]. These results suggest that CDKs are important molecular switches that contribute to cell cycle progression in parasites [30]. CDK2 plays a pivotal role in regulating G1/S and S/G2 transitions during the cell cycle[12, 13]. In A375 human melanoma cells, CRISP/Cas9 technology knockout CDK2 induces G0/G1 phase arrest and early apoptosis [31]. Gastric cancer cells culture in a low Cl^- medium inhibits cell growth and causes the G0/G1 phase arrest by diminishing the expression of CDK2 and phosphorylated tumor suppressor gene Rb [32]. In this study, the levels of *Et*CRK2 mRNA and protein in the infected/diclazuril group decreased relative to those in the infected/control group. This effect indicates that diclazuril likely blocks cell cycle in merozoites in the G1 phase by interfering with the *Et*CRK2 pathway and induces the occurrence of apoptotic events[20, 35], including decrease in mitochondrial membrane and chromatin agglutination [20], downregulation of serine/threonine protein phosphatase type 5 mRNA expression [3] and increase in glyceraldehyde-3-phosphate dehydrogenase transcription and protein expression [36]. Thus, the normal reproductive cycle of *E. tenella* is inhibited, and the number of second-generation merozoites subsequently decreases [19].

The spatial distribution of proteins affects protein function. The localisation of *T. annulata* CRK2 protein in parasite nuclei is upregulated transiently in midmerogony. This phenomenon suggests that TaCRK2 coordinated the parasite's nuclear division [17]. The protozoan *G. lamblia* CDK2 localised in the

cytoplasm contributes to cyst formation and shows increased expression during encystation [8]. The members of *P. falciparum* CDK-like kinase (CLK) family, PfCLk-1 and PfCLK-2, are primarily localised in the nucleus, and the further dispersion of PfCLK-2 into the cytoplasm indicates that PfCLKs participate in gene regulation and the post-transcriptional modification of mRNA in the malarial blood stage [37]. In the present study, *Et*CRK2 was localised in the cytoplasm of second-generation merozoites, and the fluorescence intensity of *Et*CDK2 decreased under diclazuril treatment. This phenomenon is consistent with the determined expression levels. These results implies that *Et*CRK2 plays an essential role in the asexual life cycle of *E. tenella* and using agents targeting CRK2 is potential therapeutic strategy against coccidiosis. However, the exact molecular mechanism needs to be further verified in a coccidial cell model in vitro using CDKs-specific inhibitors.

Conclusion

Our results indicate that diclazuril downregulates the mRNA and protein expression levels of *Et*CRK2 and disrupts the cell cycle of second-generation merozoites. This action may be an aspect of the molecular mechanism of the anticoccidial action of diclazuril.

Methods

Inoculum and drug

Oocysts of *E. tenella* (Luoyang strain) were passaged before inoculation, and the obtained oocysts was sporulated in 2.5% $K_2Cr_2O_7$ solution at 29 °C for 48 h. Diclazuril (> 99%; Shanghai Veterinary Research Institute, CAAS, China) was supplied at a dose of 1 mg/kg in broiler feed.

Experimental chickens and treatment

One-day-old male Chinese Yellow broiler chickens were obtained from Gonghua Commercial Hatchery, Luoyang, China. The chickens were kept in wire-floored batteries for 14 days under coccidiosis-free conditions. On the 14th day, healthy 90 chickens were randomly divided into two groups of 45 with three biological replicates of 15 in each group: (1) Chickens that were challenged with *E. tenella* sporulated oocysts and received commercial diet without drugs were included to the infected/control group. (2) Chickens that were challenged with *E. tenella* sporulated oocysts and treated with 1 mg/kg diclazuril in feed from 96 h to 120 h were included to the infected/diclazuril group. Inoculation was performed with a dose of 8×10^4 sporulated oocysts/chicken on day 14. The experimental scheme conformed strictly to the guidelines of the Institutional Animal Care and Use Committee (No. 201) of Henan University of Science and Technology (Luoyang, Henan, China).

Preparation of the second-generation merozoites

At 120 h postinoculation, chickens were killed through CO_2 asphyxiation, and the pooled caecal tissues from 10 randomly selected chickens in each replicate were used for the preparation of the second-

generation merozoites in accordance with a previously described method [19-21]. Briefly, caecal tissues were cut into pieces, then incubated with enzyme digestion solution (0.12 mol/L NaCl, 3.0 mmol/L $K_2HPO_4 \cdot 3H_2O$, 9 mmol/L $CaCl_2$, 1 mg/mL hyaluronidase, 1 mg/mL BSA and 0.02 mol/L Tris; pH = 7.4) at 37 °C for 60 min. After the filtration and centrifugation of the digestion mixture, the collected sediment was incubated with red blood cell lysis buffer (Beyotime, Shanghai) at 4 °C for 10 min. Lysates were removed through centrifugation, and the merozoites were collected through density gradient centrifugation. The collected merozoite samples were subjected to total RNA preparation, Western blot and immunofluorescence assay successively. Three samples in each group were used for each experiment.

Total RNA preparation and cDNA synthesis

The total RNA of merozoites was extracted with TRIzol® Reagent (Invitrogen, USA) according to the manufacturer's procedure, and cDNA was synthesised with EasyScript One-Step gDNA Removal and cDNA Synthesis SuperMix (TransGen Biotech, Beijing).

Amplification of the *Et*CRK2 gene

According to the sequence (GenBank: AY508221.1), specific primers P1: 5'-AAGGGACTTACGGAGTGGTTTA-3' and P2: 5'-TGAATTTACGTGAATATGTTGG-3' were designed to amplify the *Et*CRK2 gene and an ORF from a cDNA template. Amplified fragments were separated through 1% agarose gel electrophoresis and isolated using TaKaRa MiniBEST Agarose Gel DNA Extraction Kit Ver.4.0 according to the manufacturer's instructions. The purified amplified fragments were ligated into the pMD-19T vector and then transformed into *Escherichia coli* strain DH5α. The recombinant clone of pMD-19-*Et*CRK2 was identified through PCR and sequenced by Shanghai Sangon Biotech Co., Ltd. The positive plasmid was named pMD-19-*Et*CRK2.

Prokaryotic expression and purification of *Et*CRK2

Using pMD-19-*Et*CRK2 as a template, the ORF of *Et*CRK2 was amplified using primers containing *Eco*R I (P2-F: 5'-CGGGAATTCATGGAGCGCTACAAGA-3') or *Hin*d III (P2-R: 5'-TCTTGTAGCGCTCCATGAATTCCCG-3') restriction sites. Amplification products and pET-28a (+) were digested by *Eco*R I and *Hin*d III prior to ligation. The recombinant plasmid pET-28a-*Et*CRK2 was transformed into *E. coli* Rosetta (DE3) competent cells. Expression was induced at 37 °C with 0.5 mM IPTG, recombinant *Et*CRK2 (r*Et*CRK2) protein was purified through Ni-NTA His Bind Resin affinity chromatography (Novagen, Germany) and then analysed using SDS-PAGE.

Polyclonal antibody preparation

For the production of polyclonal antibodies, purified r*Et*CRK2 protein was used as an antigen in subsequent immune procedures. r*Et*CRK2 protein emulsified with the same volume of Freund's complete adjuvant (Sigma-Aldrich) was injected into New Zealand rabbits at a dose of 500 μg/rabbit. After 2

weeks, purified r*Et*CRK2 protein emulsified with Freund's incomplete adjuvant (Sigma-Aldrich) was injected to the rabbits at a dose of 500 μg/rabbit for secondary immunisation. After a 2 week hiatus, the third and fourth rounds of immunisation were performed separately. Ten days after the last immunisation, serum samples were collected for the determination of specificity antibody titer. The specificity of the antibody was determined with Western blot. Briefly, 25 ng of recombinant protein was used for SDS-PAGE, and preimmunisation rabbit serum and antiserum were used as the primary antibodies. HRP conjugated goat antirabbit IgG (Biolab, Beijing) was subsequently used. HRP activity was revealed by enhanced chemiluminescence system using BeyoECL Plus substrate (P0018S, Beyotime Biotechnology, China). The antibody titer was analysed with indirect enzyme linked immunosorbent assay (ELISA) [38]. Briefly, 500 ng/well r*Et*CRK2 protein was used to coat 96-well plates at 4 °C overnight, and the antiserum diluted with PBS at 1:2K, 1:4K, 1:8K, 1:16K, 1:32K, 1:64K, 1:128K, 1:256K, 1:512K, 1:1024K and 1:2048K were incubated with the antigen at 37 °C for 2 h. After washing with TBST, horse radish peroxidase (HRP)-conjugated goat antirabbit IgG were added to all microwells at 37 °C for 2 h. After washing, the substrate solution tetramethylbenzidine was added, and the microplate was read at 450 nm in a microplate reader (Multiskan FC, Thermo Scientific, USA). Preimmunisation rabbit serum and PBS were used as the control.

*Et*CRK2 mRNA expression analysis

The mRNA expression level of *Et*CRK2 was quantified through real-time PCR with a CFX96 touch real-time PCR system (Bio-Rad, America) and TB Green® *Premix Ex Taq*™ GC (Perfect Real Time; Takara, Beijing). Each reaction was performed in triplicate, and the entire experiment was carried out in triplicate. *E. tenella* 18S rRNA was used as the control. The primer sequences are shown in Table 1. Relative mRNA expression was determined using the $^{\Delta\Delta}$Ct method.

Western blot analysis

Purified merozoites were treated with RIPA lysis buffer (Beyotime, Shanghai) for Western blot analysis and determined using a BCA protein assay kit (Cwbio, Beijing) for concentration assessment. Pyrolysis products were dissolved in SDS-PAGE sample buffer (Beyotime, Shanghai), heated at 96 °C for 5 min, separated on 12% SDS-PAGE and electrotransferred to a polyvinylidene difluoride membrane (Membrane Solutions, USA). The membrane was detected with rabbit antiserum against *Et*CRK2 as the primary antibody or anti-β-tubulin monoclonal antibody (1:1000 dilution, K200059 M, Solarbio, China), followed by HRP conjugated goat antirabbit IgG ((Biolab, Beijing). HRP activity was revealed by enhanced chemiluminescence system using BeyoECL Plus substrate (P0018S, Beyotime Biotechnology, China) and Image J Software. The independent experiments were performed in triplicate.

Immunofluorescence test

In accordance with our previously described method with minor modifications [22], the merozoites were prepared into smears and fixed with 4% paraformaldehyde. The merozoites were washed three times with PBS, then permeabilised with 1% Triton X-100 (Sangon-Biotech, Shanghai) and blocked with 2% BSA-PBS

at 4 °C overnight. Rabbit antiserum against *Et*CRK2 (1:2000 dilution) was used as the primary antibody at 37 °C for 1 h, and FITC-conjugated goat antirabbit IgG (Servicebio, Wuhan) with 1:100 dilution was used as the second antibody at 37 °C in the dark for 1 h. Finally, the merozoites were stained with 4',6'-diamidino-2-phenylindole (Boster, China) at room temperature for 30 min, and 50 μL of anti-fade mounting medium (Sangon Biothch, Shanghai) was used to close the coverslip. Images were visualised with a confocal laser scanning microscope (LSM 800, ZEISS) at a $l_{ex/em}$ of 492 nm/520 nm and 358 nm/461 nm.

Statistical analysis

Data were expressed as mean ± standard deviation. Student's *t* test was used in statistical analyses. Values of $P < 0.05$ and $P < 0.01$ were considered significant.

Abbreviations

CDK: Cyclin-dependent kinases; CRK: CDK-related kinase; PCR: Polymerase chain reaction; bp: base pair; ORF: Open reading frame; IPTG: Isopropyl-b-D-thiogalactopyranoside; SDS-PAGE: Sodium dodecyl sulfate-polyacrylamide gel electrophoresis; kDa: Kilodalton; ELISA: indirect enzyme linked immunosorbent assay. PBS: Phosphate buffer saline; TBST: Tris-Buffered Saline containing 0.05% Tween 20; BSA: Bovine serum albumin; FITC: Fluoresceine isothiocyanate; *E. tenella*: *Eimeria tenella*; *T. gondii*: *Toxoplasma gondii*; *P. falciparum*: *Plasmodium falciparum*; *P. berghei*: *Plasmodium berghei*.

Declarations

Ethics approval and consent to participate

Animals housing and care complied with the Guide for Ethical Review of laboratory animal welfare, China (GB/T 35892-2018). The study was approved by the Institutional Animal Care and Use Committee of Henan University of Science and Technology.

Consent for publication

Not applicable.

Availability of data and materials

The data generated or analyzed during this study are included in this article.

Competing interests

No potential conflict of interest was reported by the authors.

Funding

This research was funded by National Natural Science Foundation of China (Grants

Nos. 31101855 and 31472238) and Natural Science Foundation of Henan (Grant No. 202300410120). This funding body provided monetary support only and did not have any input into the design of the study, collection, analysis, and interpretation of data.

Authors' contributions

BZ: Software, Validation, Formal analysis, Data Curation, Methodology, Visualization,

Writing - Review & Editing, Funding acquisition. HD: Writing-Original Draf, Visualization, Investigation. JY, JC, HG and ET: Investigation. All authors read and

approved the final version of the manuscript.

Acknowledgements

Not applicable.

Authors' information

Dr. Bian-hua Zhou, E-mail: zhoubh@haust.edu.cn

Mrs. Hai-yan Ding, E-mail: dinghy@stu.haust.edu.cn

Mrs. Jing-yun Yang, E-mail: YangJingyun@stu.haust.edu.cn

Mr. Jun Chai, E-mail: chaijun@lypt.edu.cn

Mr. Hong-wei Guo, E-mail: guohongwei@hnuahe.edu.cn

Dr. Er-jie Tian, E-mail: tej1212@haust.edu.cn

References

1. Zhou BH, Jia LS, Wei SS, Ding HY, Yang JY, Wang HW. Effects of *Eimeria tenella* infection on the barrier damage and microbiota diversity of chicken cecum. Poultry science. 2020;99(3):1297-1305.
2. Tan L, Li Y, Yang X, Ke Q, Lei W, Mughal MN, et al. Genetic diversity and drug sensitivity studies on *Eimeria tenella* field isolates from Hubei Province of China. Parasites & vectors. 2017;10(1):137.
3. Zhou BH, Wang HW, Zhao ZS, Liu M, Yan WC, Zhao J, et al. A novel serine/threonine protein phosphatase type 5 from second-generation merozoite of *Eimeria tenella* is associated with diclazuril-induced apoptosis. Parasitology research. 2013;112(4):1771-1780.
4. Fernández MLS, Engels KK, Bender F, Gassel M, Marhöfer RJ, Mottram JC, et al. High-throughput screening with the *Eimeria tenella* CDC2-related kinase2/cyclin complex EtCRK2/EtCYC3a.

Microbiology (Reading, England). 2012;158(Pt 9):2262-2271.

5. Engels K, Beyer C, Suárez Fernández ML, Bender F, Gassel M, Unden G, et al. Inhibition of *Eimeria tenella* CDK-related kinase 2: From target identification to lead compounds. ChemMedChem. 2010;5(8):1259-1271.
6. Lim S, Kaldis P. Cdks, cyclins and CKIs: roles beyond cell cycle regulation. Development (Cambridge, England). 2013;140(15):3079-3093.
7. Deshmukh AS, Agarwal M, Dhar SK. Regulation of DNA replication proteins in parasitic protozoans: possible role of CDK-like kinases. Current genetics. 2016;62(3):481-486.
8. Cho CC, Su LH, Huang YC, Pan YJ, Sun CH. Regulation of a Myb transcription factor by cyclin-dependent kinase 2 in *Giardia lamblia*. The Journal of biological chemistry. 2012;287(6):3733-3750.
9. Malumbres M. Cyclin-dependent kinases. Genome biology. 2014;15(6):122.
10. Hydbring P, Malumbres M, Sicinski P. Non-canonical functions of cell cycle cyclins and cyclin-dependent kinases. Nature reviews Molecular cell biology. 2016;17(5):280-292.
11. García-Reyes B, Kretz AL, Ruff JP, von Karstedt S, Hillenbrand A, Knippschild U, et al. The emerging role of cyclin-dependent kinases (CDKs) in pancreatic ductal adenocarcinoma. International journal of molecular sciences. 2018;9(10).
12. Li Y, Zhang J, Gao W, Zhang L, Pan Y, Zhang S, et al. Insights on structural characteristics and ligand binding mechanisms of CDK2. International journal of molecular sciences. 2015;16(5):9314-9340.
13. Peng C, Zeng W, Su J, Kuang Y, He Y, Zhao S, et al. Cyclin-dependent kinase 2 (CDK2) is a key mediator for EGF-induced cell transformation mediated through the ELK4/c-Fos signaling pathway. Oncogene. 2016;35(9):1170-1179.
14. Alvarez CA, Suvorova ES. Checkpoints of apicomplexan cell division identified in *Toxoplasma gondii*. PLoS pathogens. 2017;13(7):e1006483.
15. Halbert J, Ayong L, Equinet L, Le Roch K, Hardy M, Goldring D, et al. A *Plasmodium falciparum* transcriptional cyclin-dependent kinase-related kinase with a crucial role in parasite proliferation associates with histone deacetylase activity. Eukaryotic cell. 2010;9(6):952-959.
16. Balestra AC, Zeeshan M, Rea E, Pasquarello C, Brusini L, Mourier T, et al. A divergent cyclin/cyclin-dependent kinase complex controls the atypical replication of a malaria parasite during gametogony and transmission. Elife. 2020;9:e56474.
17. Kinnaird J, Logan M, Tait A, Langsley G. TaCRK3 encodes a novel *Theileria annulata* protein kinase with motifs characteristic of the family of eukaryotic cyclin dependent kinases: a comparative analysis of its expression with TaCRK2 during the parasite life cycle. Gene. 2001;279(2):127-135.
18. Kinnaird JH, Bumstead JM, Mann DJ, Ryan R, Shirley MW, Shiels BR, et al. EtCRK2, a cyclin-dependent kinase gene expressed during the sexual and asexual phases of the *Eimeria tenella* life cycle. International journal for parasitology. 2004;34(6):683-692.
19. Zhou BH, Wang HW, Wang XY, Zhang LF, Zhang KY, Xue FQ. *Eimeria tenella*: effects of diclazuril treatment on microneme genes expression in second-generation merozoites and pathological

changes of caeca in parasitized chickens. Experimental parasitology. 2010;125(3):264-270.

20. Zhou B, Wang H, Xue F, Wang X, Fei C, Wang M, et al. Effects of diclazuril on apoptosis and mitochondrial transmembrane potential in second-generation merozoites of *Eimeria tenella*. Veterinary parasitology. 2010;168(3-4):217-222.
21. Zhou BH, Ding HY, Yang JY, Chai J, Guo HW, Wang HW. Effects of diclazuril on the expression of enolase in second-generation merozoites of *Eimeria tenella*. Poultry science. 2020;99(12):6402-6409.
22. Zhou BH, Jia LS, Guo HW, Ding HY, Yang JY, Wang HW. Eukaryotic elongation factor 2 is involved in the anticoccidial action of diclazuril in the second-generation merozoites of *Eimeria tenella*. Veterinary parasitology. 2019;276:108991.
23. Tian EJ, Zhou BH, Wang XY, Zhao J, Deng W, Wang HW. Effect of diclazuril on intestinal morphology and SIgA expression in chicken infected with *Eimeria tenella*. Parasitology research. 2014;113(11):4057-4064.
24. Zhou BH, Liu LL, Liu J, Yuan FW, Tian EJ, Wang HW. Effect of diclazuril on the bursa of fabricius morphology and SIgA expression in chickens infected with *Eimeria tenella*. The Korean journal of parasitology. 2015;53(6):675-682.
25. Wang X, Zou W, Yu H, Lin Y, Dai G, Zhang T, et al. RNA sequencing analysis of chicken cecum tissues following *Eimeria tenella* infection in vivo. Genes. 2019;10(6).
26. Mottram JC, Smith G. A family of trypanosome cdc2-related protein kinases. Gene. 1995;162(1):147-152.
27. Roques M, Wall RJ, Douglass AP, Ramaprasad A, Ferguson DJ, Kaindama ML, et al. Plasmodium p-type cyclin CYC3 modulates endomitotic growth during oocyst development in mosquitoes. PLoS pathogens. 2015;11(11):e1005273.
28. Deshmukh AS, Mitra P, Kolagani A, Gurupwar R. Cdk-related kinase 9 regulates RNA polymerase II mediated transcription in *Toxoplasma gondii*. Biochimica et biophysica acta Gene regulatory mechanisms. 2018;1861(6):572-585.
29. Vinkenoog R, Sperança MA, Ramesar J, Thomas AW, del Portillo HA, Janse CJ, et al. Characterisation of the Cdc2-related kinase 2 gene from *Plasmodium knowlesi* and *P. berghei*. Molecular and biochemical parasitology. 1998;95(2):229-240.
30. Iwanaga T, Sugi T, Kobayashi K, Takemae H, Gong H, Ishiwa A, et al. Characterization of *Plasmodium falciparum* cdc2-related kinase and the effects of a CDK inhibitor on the parasites in erythrocytic schizogony. Parasitology international. 2013;62(5):423-430.
31. Liu H, Li Z, Huo S, Wei Q, Ge L. Induction of G0/G1 phase arrest and apoptosis by CRISPR/Cas9-mediated knockout of CDK2 in A375 melanocytes. Molecular and clinical oncology. 2020;12(1):9-14.
32. Shiozaki A, Otsuji E, Marunaka Y. Intracellular chloride regulates the G(1)/S cell cycle progression in gastric cancer cells. World journal of gastrointestinal oncology. 2011;3(8):119-122.
33. Ganter M, Goldberg JM, Dvorin JD, Paulo JA, King JG, Tripathi AK, et al. *Plasmodium falciparum* CRK4 directs continuous rounds of DNA replication during schizogony. Nature microbiology. 2017;2:17017.

34. Gray KA, Gresty KJ, Chen N, Zhang V, Gutteridge CE, Peatey CL, et al. Correlation between cyclin dependent kinases and artemisinin-induced dormancy in *Plasmodium* falciparum In vitro. PloS one. 2016;11(6):e0157906.
35. Lee KM, Lee K, Choi YK, Choi YJ, Seo HS, Ko SG. SH003-induced G1 phase cell cycle arrest induces apoptosis in HeLa cervical cancer cells. Molecular medicine reports. 2017;16(6):8237-8244.
36. Wang C, Han C, Li T, Yang D, Shen X, Fan Y, et al. Nuclear translocation and accumulation of glyceraldehyde-3-phosphate dehydrogenase involved in diclazuril-induced apoptosis in *Eimeria tenella* (*E. tenella*). Veterinary research. 2013;44(1):29.
37. Agarwal S, Kern S, Halbert J, Przyborski JM, Baumeister S, Dandekar T, et al. Two nucleus-localized CDK-like kinases with crucial roles for malaria parasite erythrocytic replication are involved in phosphorylation of splicing factor. Journal of cellular biochemistry. 2011;112(5):1295-1310.
38. Gan SD, Patel KR. Enzyme immunoassay and enzyme-linked immunosorbent assay. The Journal of investigative dermatology. 2013;133(9):e12.

Tables

Table 1 Primer sequences with their corresponding PCR product size and position

Gene	Primers (5′→3′)	Primer locations	Product (base pairs)	Genbank Accession No.
18S rRNA	ATCGCAGTTGGTTCTTTTGG CCTGCTGCCTTCCTTAGATG	248-417	170	U67121
*Et*CRK2	CTAGACGACTGCCGACCTTC GGGTTCCGTCTCTGCTTATG	524-746	223	AY508221.1

Figures

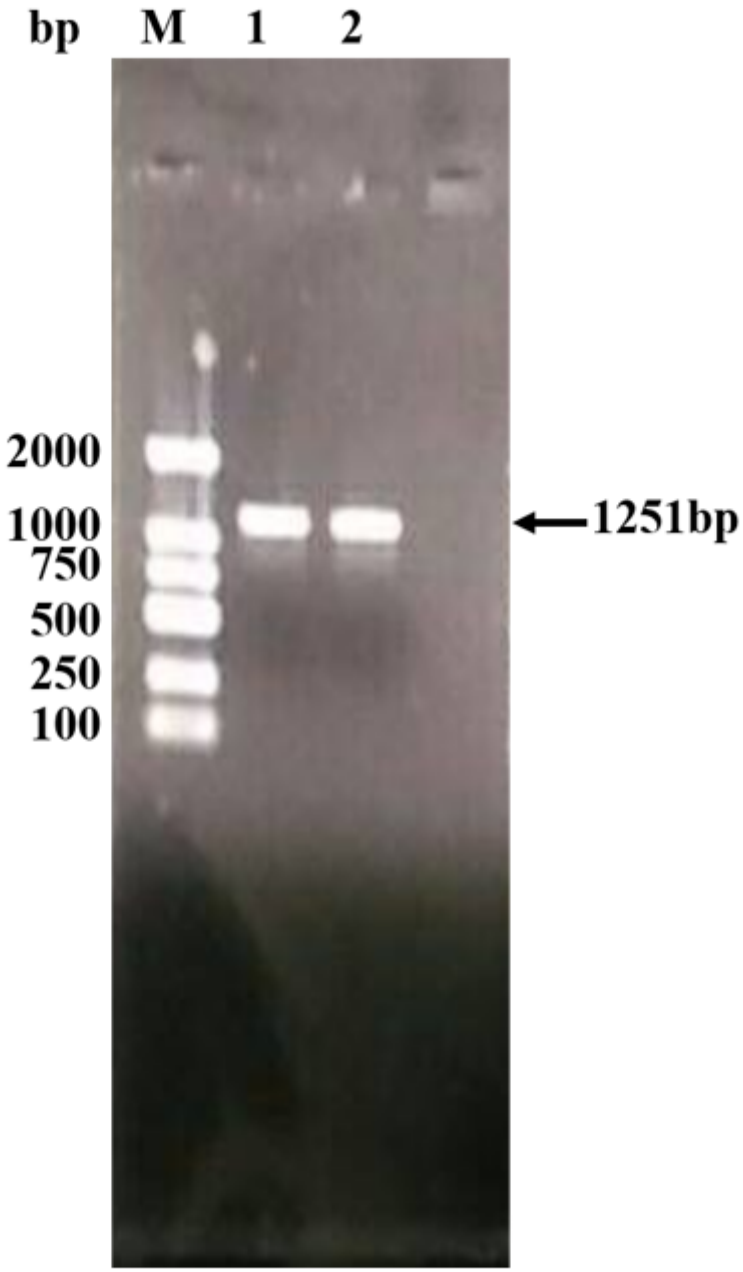

Figure 1

Agarose gel electrophoresis of pET-28a-EtCRK2 ligation. M, DL2000 DNA Marker; 1and 2, PCR amplification products via pET-28a (+) vector universal primers.

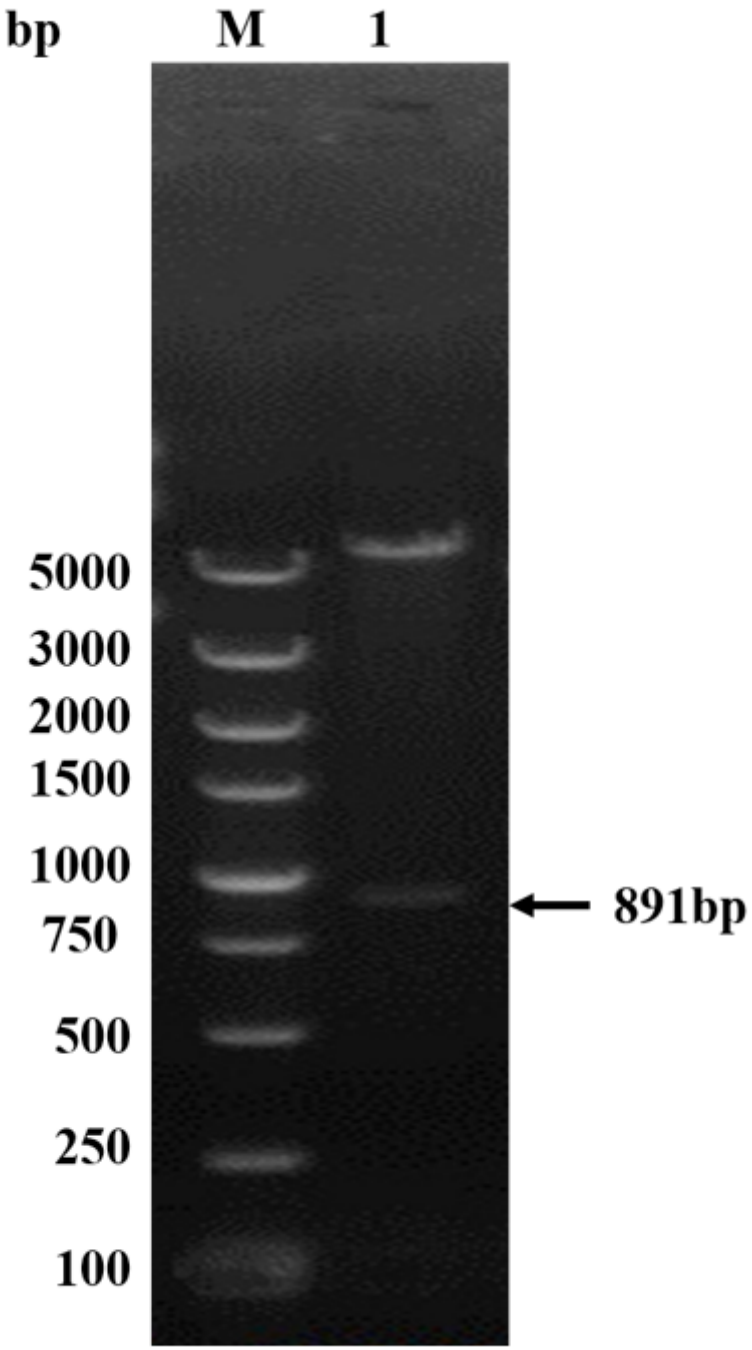

Figure 2

Restriction digestion analysis of pET-28a-EtCRK2. M, DL5000 DNA Marker; 1, Plasmid pET-28a-EtCRK2 digested by EcoR I and Hind III.

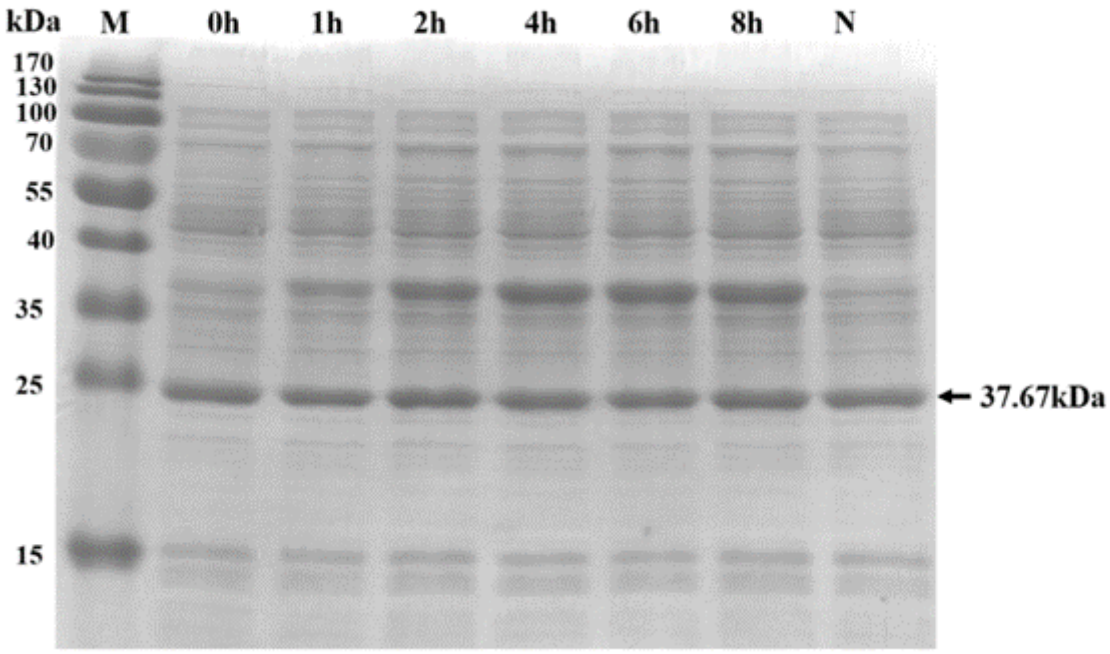

Figure 3

SDS-PAGE analysis of induced expression of EtCRK2 fusion protein. M, Protein molecular weight Marker; pET-28a-EtCRK2 were induced expression of 1, 2, 4, 6 and 8 h successively; N, empty pET-28a vector were induced expression.

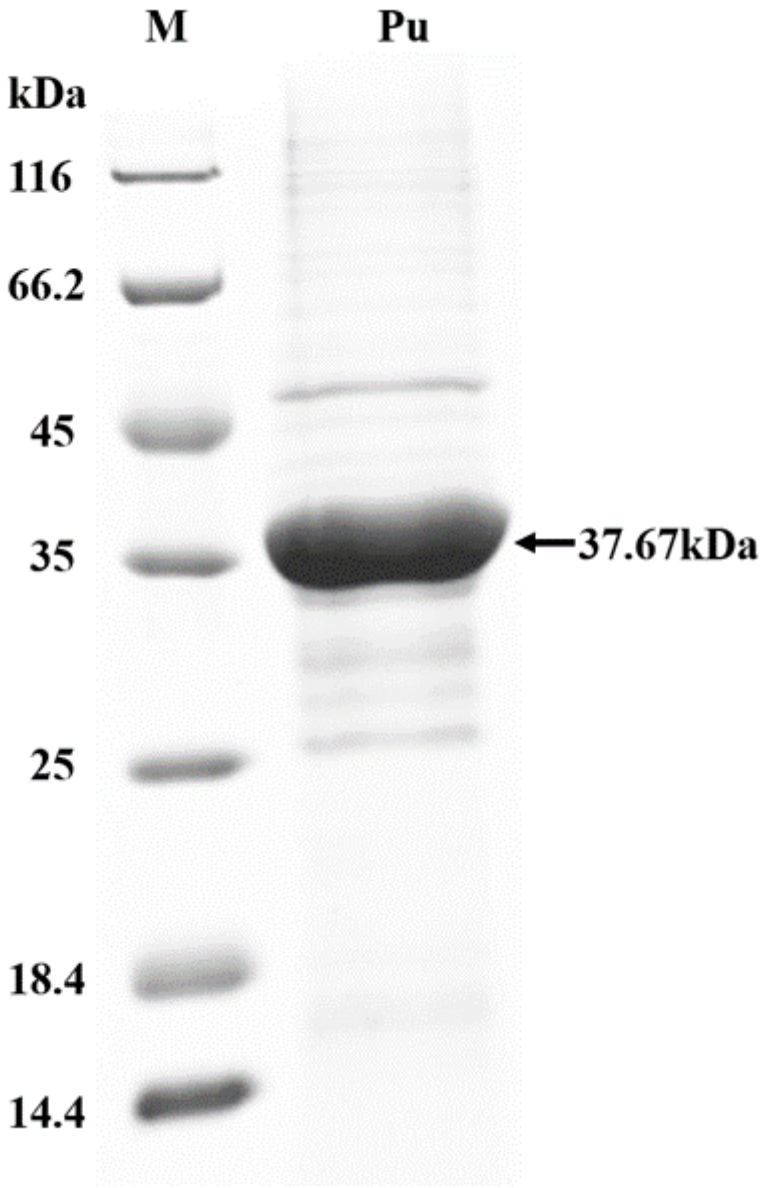

Figure 4

Purification of rEtCRK2 protein. M, Protein molecular weight Marker; Pu, purified rEtCRK2 protein.

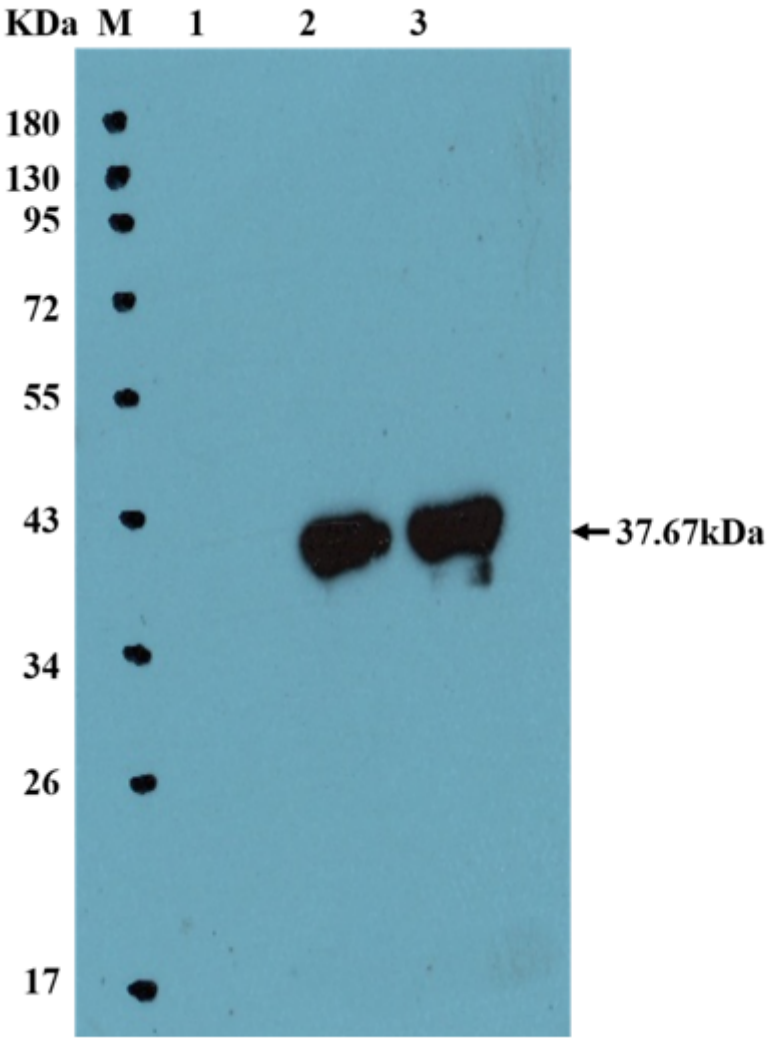

Figure 5

Rabbit-anti-EtCRK2 serum specific binding analysis by Western blot. M, Protein molecular weight Marker; 1, Preimmunisation serum as the first antibody; 2 and 3, antiserum as the first antibody.

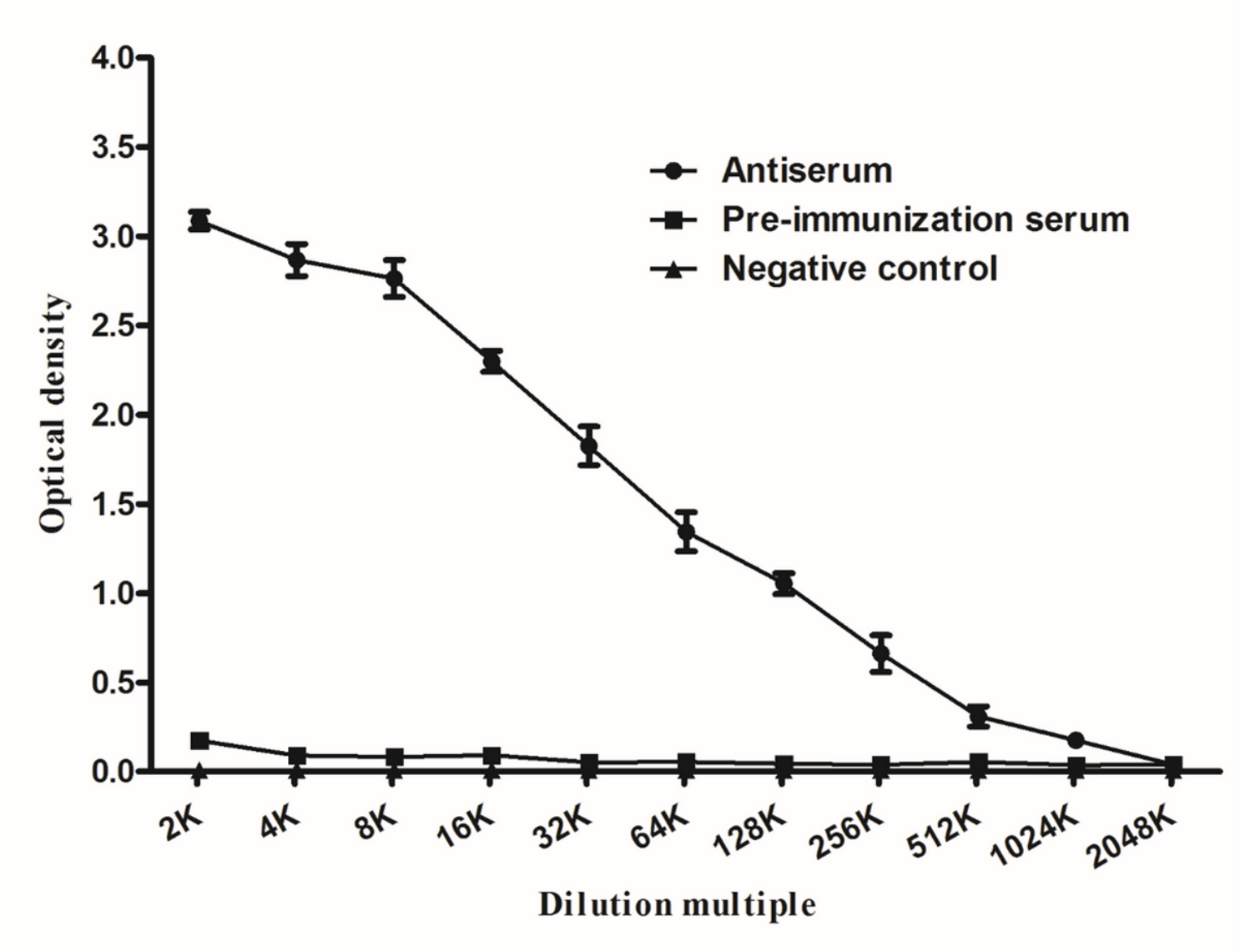

Figure 6

Serum anti-EtCRK2 antibody levels measured by ELISA. The titer of antibody exceeded 512K.

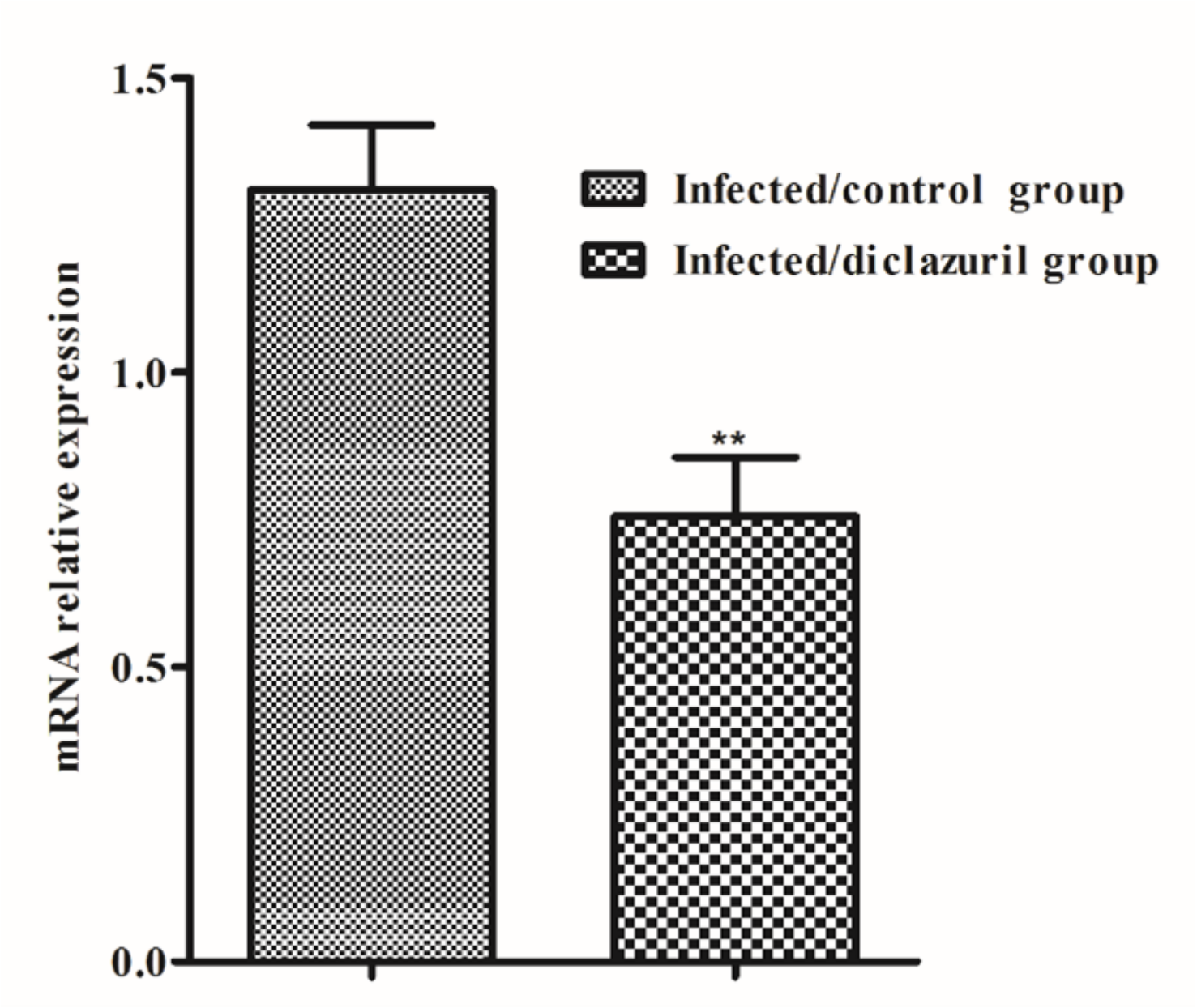

Figure 7

mRNA relative expression level of EtCRK2. mRNA expression in infected/diclazuril group was downregulated compared with that in the infected/control group.

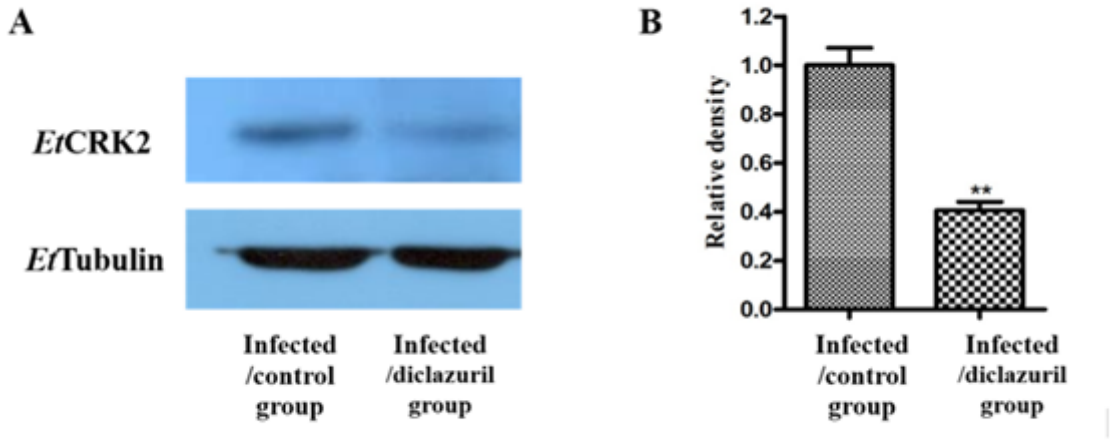

Figure 8

Western blot analysis of EtCRK2 protein expression. A, Western blot electrophoretic pattern of EtCRK2 and EtTubulin. B, EtCRK2 relative density. ** P 0.01 compared with the infected/control group.

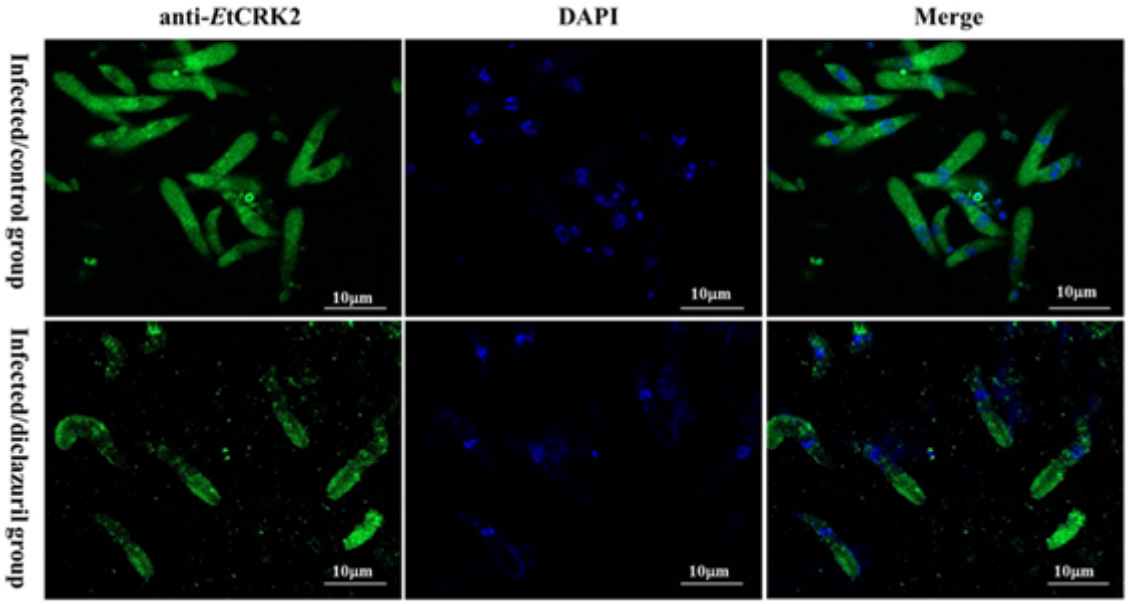

Figure 9

Localisations of EtCRK2 in second-generation merozoites. EtCRK2 is widely distributed to the cytoplasm in merozoite. Compared with the infected/control group, the EtCRK2 immunostaining staining was significantly weaker in the merozoite of the infected/diclazuril group.

Supplementary Files

This is a list of supplementary files associated with this preprint. Click to download.

- Riginalimages.docx
- NC3RsARRIVEGuidelinesChecklistfillable.pdf